JOURNAL OF AIRCRAFT
Vol. 44, No. 1, January–February 2007

Robust Design of an Aerodynamic Compensation Pitot-Static Tube for Supersonic Aircraft

A. Latif,* J. Masud,† S. R. Sheikh,‡ and K. Pervez§
National University of Sciences and Technology, Risalpur 24090, Pakistan

DOI: 10.2514/1.22775

We have designed an aerodynamic compensation pitot-static tube that improves upon the traditional ogival pitot-static tube. The proposed design is able to provide the desired compensation in both subsonic (negative value of the pressure coefficient *Cp*) and supersonic (zero value of *Cp*) regimes at the same axial location. At this axial location, the local *Cp* gradient is small in the subsonic regime and is close to zero in the supersonic regime so that in practical application, this pitot-static tube would perform better than an ogival pitot-static tube. The proposed design can be used effectively to compensate for *Cp* position errors of up to +0.1 in the subsonic regime, by nondimensional stretching of the basic profile, while maintaining zero *Cp* in the supersonic regime. Computational fluid dynamics is used in the design and analysis of the proposed pitot-static tube. The complete Mach number regime (Mach less than two) has been computationally analyzed for different profiles resulting from stretching of the basic profile, to validate the proposed design's capability. A design methodology is also presented in which a specific pitot-static tube profile can be extracted from the general nondimensional profile to aerodynamically compensate for a known position error in *Cp*.

Nomenclature

Cp	=	pressure coefficient $(P - P_\infty)/\frac{1}{2}\rho_\infty V_\infty^2$
$D_{\max}$	=	maximum diameter of the compensation region
f	=	fineness ratio $(X_{\max}/D_{\max})$
M	=	freestream Mach number
P	=	static pressure
P_t	=	total pressure
P_∞	=	freestream static pressure
V_∞	=	freestream velocity
$X_{\max}$	=	maximum length of the compensation region
x	=	axial coordinate
$Y_{\max}$	=	maximum radial thickness of the compensation region $(D_{\max}/2)$
y	=	radial coordinate
y^+	=	nondimensional length scale associated with the turbulence model
β	=	sideslip angle
ρ_∞	=	freestream density

I. Introduction

THE aircraft pitot-static tube (subsequently referred to as the pitot tube) is one of the important air data sensors and is designed to measure correct ambient static and total pressure corresponding to aircraft flight conditions. These pressure measurements translate into aircraft speed, pressure altitude, Mach number, vertical velocity information, etc., all of which are necessary for multiple aircraft subsystems such as the flight control system, avionics/weapons subsystems, the engine control subsystem and cockpit flight instruments, etc. The measurement of correct ambient (atmospheric) static pressure by the pitot tube over the whole Mach number regime (subsonic to supersonic) of the aircraft is the most critical aspect in its design [1]. Generally, a pitot tube is placed ahead of the aircraft, where the local static pressure in the subsonic regime is higher than the ambient static pressure (i.e., positive Cp value [1,2]) and is referred to as the Cp position error. In the supersonic regime, the local static pressure ahead of the aircraft equals the ambient static pressure (i.e., Cp position error value is zero). An aerodynamic compensation pitot tube is designed to compensate for the position error by generating opposite local Cp by a carefully contoured profile [1,3–5], as shown in Fig. 1. This presents multiple challenges to the designer, due to the inherently different nature of subsonic and supersonic flows. An ideal pitot tube would fully compensate for the aircraft presence and, thus, the static pressure measured by it over the whole flight regime, subsonic through supersonic, would be the corresponding atmospheric (ambient) pressure.

Older-generation supersonic aircraft generally used a non-compensating pitot tube with associated static pressure measurement errors in the subsonic regime [1]. A common aerodynamic compensation pitot tube has an ogival shape that is based on a profile formed by a quadratic polynomial [1,3]. This kind of pitot tube is used on some modern supersonic aircraft. A feature of such a pitot tube is a significant gradient of the surface Cp near its zero value in the supersonic regime, as shown in Fig. 2. Additionally, the zero Cp point also shifts axially with supersonic Mach number. These features of the surface Cp behavior make the ogival pitot tube quite sensitive to static port location as well as manufacturing tolerances. An approximate solution to this undesirable feature is either through manipulation of static pressure measured at axially distributed pressure ports on the surface of the pitot tube or by accepting some inherent error in measured Cp in the supersonic regime that is partially corrected by an air data computer.

The surface Cp distribution in the compensation region is a strong function of its shape or profile; therefore, the possibility exists of improving or modifying the Cp distribution by modifying the pitot tube shape. It is relatively simple to get desired compensation characteristics in the subsonic region by using a particular compensation region profile [1] and in the supersonic region by using a different profile [1]. The challenge to the designer arises once the same pitot tube is required to work well in both subsonic and supersonic regimes. Because of this aspect, the research literature [1,3–5] typically focuses on relatively simple compensation region

Presented as Paper 1385 at the 44th AIAA Aerospace Sciences Meeting and Exhibit, Reno, NV, 9–12 January 2006; received 27 January 2006; revision received 28 August 2006; accepted for publication 16 October 2006.

*Graduate Student, Department of Aerospace Engineering, College of Aeronautical Engineering.
†Associate Professor Department of Aerospace Engineering, College of Aeronautical Engineering.
‡Professor, Head, Department of Aerospace Engineering, College of Aeronautical Engineering.
§Professor, Dean, College of Aeronautical Engineering. Member AIAA.

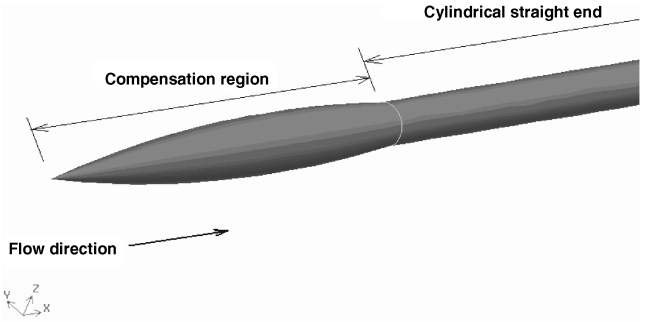

Fig. 1 Aerodynamic compensation pitot tube having an ogival (quadratic) compensation region profile.

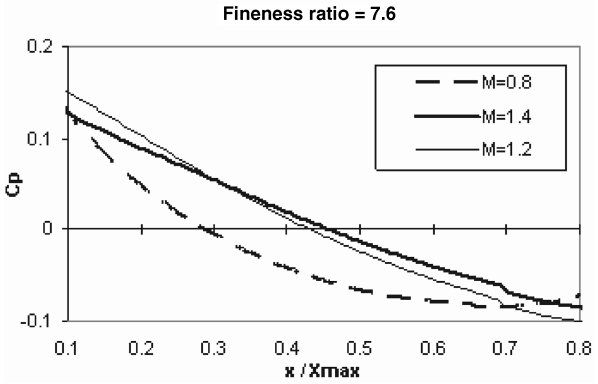

Fig. 2 *Cp* distribution on the surface of a pitot tube having an ogival (quadratic) compensation region.

profiles, such as the ogival pitot tube (Fig. 1); consequently, such pitot tubes are being used on a number of modern supersonic aircraft. The published literature on aerodynamic compensation pitot tubes is practically devoid of novel profiles that improve upon the Cp characteristics of the ogival pitot tube, whereas present-day computational capability affords an opportunity to design better aerodynamic compensation pitot tubes.

The aim of the present study is to develop a robust compensation region profile (nondimensional) by computational fluid dynamics (CFD) analysis that has better surface Cp characteristics than an ogival pitot tube in the supersonic regime (i.e., negligible gradient near zero Cp value), while maintaining adequate subsonic compensation characteristics. The proposed design pitot tube can then be used for specific aircraft applications by simply "stretching" the nondimensional profile to achieve the desired level of compensation in the subsonic regime, while maintaining near-zero compensation in the supersonic regime.

II. Development Methodology of Proposed Compensation Region Profile

The development of a new compensation region profile is challenging, due to stringent Cp characteristics requirements in the supersonic regime, as discussed earlier. An element of trial and error is also present in compensated pitot tube design for specific applications that is apparent from earlier studies [4,5]. We started the proposed compensation region development work by first evaluating the characteristics of an ogival pitot tube having a compensation region defined by a quadratic polynomial (Figs. 1 and 2). The compensation region was then simplified by breaking it down into three conical segments, as shown in Fig. 3. The use of three conical segments in the arrangement shown in Fig. 3 results in flow compression at the tip of the first conical segment, then expansion at the junction of the first and second conical segments, and, finally, expansion again at the junction of the second and third conical segments. This sequence of flow compression–expansion–expansion in the vicinity of the simplified compensation region

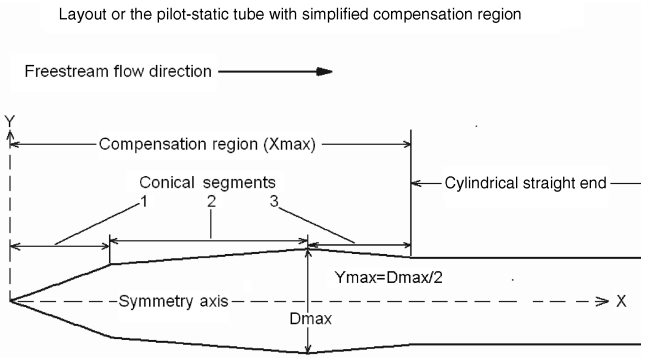

Fig. 3 Layout of the pitot tube.

occurs in both the subsonic and supersonic regimes. The surface Cp distribution of the middle conical segment (segment 2 in Fig. 3) was targeted to have negative value in the subsonic regime, with zero somewhere along its length in the supersonic regime. This was achieved by controlling the level of flow compression (segment 1 in Fig. 3) and flow expansion (the junctions of segments 1 and 2 and segments 2 and 3 in Fig. 3) by choosing various relative lengths and half-cone angles of the three conical segments. The choice of relative lengths and half-cone angles of the three conical segments (Fig. 3) were restricted such that under all freestream conditions, the compression–expansion–expansion sequence of flow near the compensation region is achieved. In this process, we created a number of simplified compensation region profiles by qualitative application of conical shock theory [6,7] in the supersonic regime. The surface Cp characteristics of these simplified pitot tubes were computationally evaluated. The pitot tubes that did not meet the middle conical segment targeted criteria, as discussed earlier, were discarded. The surface Cp characteristics of the pitot tubes that did meet the targeted criteria were compared, and the most promising one was fine-tuned by small adjustments of the conical segments parameters (relative lengths and half-cone angles). The fine-tuned arrangement of the three conical segments (represented to scale in Fig. 3) was subjected to profile smoothing refinement.

The simplified compensation region (Fig. 3) refinement process involved better representation of the compensation region by a higher-order polynomial, which closely followed the conical segment profile, while smoothing out the sharp edges created at the junction of the conical segments. This general smoothing of the compensation region profile diffused the rapid pressure changes at the junction of the conical segments and modified the surface Cp characteristics in a favorable manner (discussed later in this paper). In this process, various coefficients of the higher-order polynomial needed minor adjustments before the required surface Cp characteristics were achieved. We verified the capability of this proposed (refined) compensation region profile to compensate for a wide range of position error by stretching the basic nondimensional profile (having different fineness ratios) and computationally evaluated its characteristics for a range of subsonic and supersonic Mach numbers.

The details of the various aspects of the development methodology of the proposed compensation region profile are discussed later in this paper.

III. Computational Setup

The pitot tube is symmetric about its longitudinal axis; therefore, steady-state, 2-D axisymmetric analysis is done to evaluate its aerodynamic characteristics. This corresponds to zero angle of attack (AOA) and zero sideslip angle of the pitot tube during flight. Aircraft pitot tubes are generally oriented such that these flow conditions (AOA $= \beta = 0$) prevail in their vicinity during most parts of aircraft flight. Nonzero AOA and β effect the azimuthal location of static pressure ports [1], which can be determined after the pitot tube profile is finalized [1]. For CFD analysis, the rear end of the pitot tube, aft of the compensation region, is modeled as a straight axisymmetric

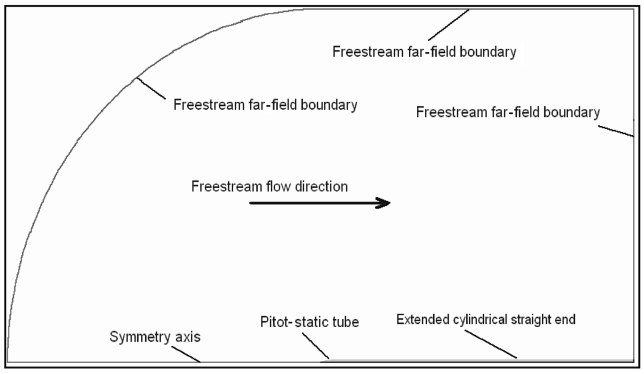

Fig. 4 Layout of the 2-D axisymmetric computational domain.

circular cylinder. The coordinate system and other parameters of the modeled pitot tube are shown in Fig. 3. In addition to the tube, the complete flow domain is modeled and shown in Fig. 4. The flow domain includes the freestream far field, the pitot tube, and the symmetry axis. The far-field boundary is placed 100 times the pitot tube maximum radius away, because placing it even 200 times away did not produce any change in the computed Cp on pitot tube surface. Modeling the far field in this manner simulates actual flight conditions. The cylindrical straight end (Figs. 3 and 4) of the pitot tube was extended till the end of the domain to avoid the influence of the rear shape on the computed surface Cp in the compensation region at subsonic Mach numbers. In all of our analysis, only the compensation region profile was modified and the rest of the computational domain was left unchanged for both subsonic and supersonic computations.

Mapped quadrilateral elements were used to mesh the computational domain. Elements were graded toward the surface of the pitot tube to accurately resolve the flow phenomena in the vicinity of the pitot tube. The computational mesh near the pitot tube compensation region is shown in Fig. 5.

We used Fluent® finite volume based CFD code [8] and its preprocessor, [9] Gambit®, for the present study. The steady, compressible Reynolds-averaged Navier–Stokes (RANS) system of equations with variable property air was solved using the coupled-implicit formulation of Fluent. A no-slip velocity boundary condition was enforced at the surface of the pitot tube, whereas a pressure far-field boundary condition [10] was used for the freestream far field, as indicated in Fig. 4. A symmetry boundary condition [10] was specified on the symmetry axis. The thermal problem was not of paramount importance in the present study, therefore, the pitot tube surface was modeled as thermally insulated.

A. Turbulence Modeling

The two-equation standard K-ε (SKE) turbulence model with standard wall treatment (law of the wall) was used for 2-D analysis [10–12]. However, we also used the one-equation Spalart–Allmaras (SA) model [10,13] to determine the sensitivity of computed results to the turbulence model. For the present study, it was found that the surface Cp in the compensation region did not change beyond 1% with either the SKE or SA turbulence models. Therefore, all the computed results presented in this study are based on the SKE turbulence model.

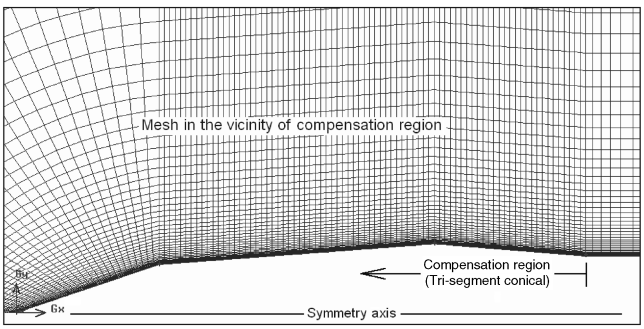

Fig. 5 Computational mesh with mapped elements.

B. Grid-Independence Analysis

Numerically computed results change with the type and density of mesh/grid used for computations. We used three different grids (grid 1, grid 2, and grid 3) to compute cases at $M = 0.6$ and 1.4. Grid 1 had 6615 elements (6808 nodes), grid 2 had 13,230 elements (13,468 nodes), and grid 3 had 26,460 elements (26,845 nodes). The results indicate a large difference in the computed surface Cp between grid 1 and grid 2. However, a percentage change of less than 1% in computed values of the surface Cp was found in the compensation region between the results of grid 2 and grid 3 for both subsonic and supersonic Mach numbers. The value of computed turbulent law y^+ remains below 87 and 104 at subsonic and supersonic speeds, respectively, for both grids 2 and 3. These values of turbulent y^+ are within normal range [11] and show reasonable resolution of the grid near the pitot tube walls [10,11]. Therefore, the results presented in this study were computed using grid 2 of 13,230 elements (13,468 nodes) or better. Part of grid 2 in the vicinity of the compensation region is shown in Fig. 5.

C. Verification of Computational Technique and Results

The flowfield in the vicinity of the pitot tube at zero AOA and β (axisymmetric case) is relatively straightforward (discussed later) without wakes, separation regions, or recirculating flow. Computation of such flowfield is one of the simpler aerodynamic problems. The CFD software package used in the present study (Fluent [8]) is well established in the CFD community, and the accuracy of its results has been verified for a number of complex problems [10].

For verification of the computational technique and results presented in this paper, sample computed results for a representative pitot tube are compared with as-yet-unpublished wind-tunnel tests results, as shown in Fig. 6. These wind-tunnel tests (WTT) were done at a 0.6×0.6 m cross-sectional high-speed wind tunnel using a 1:1 scale pitot tube. The comparison (Fig. 6) shows good agreement in the subsonic regime and reasonable agreement in the supersonic regime. In the transonic regime, the surface pressure behavior for a real pitot tube is sensitive to tolerances (errors) in pitot tube compensation region profile, static pressure ports locations, and its alignment in the wind tunnel. This sensitivity is mainly due to formation of initial shock waves at uncertain locations (combined effect of tolerances and alignment) on the surface of the pitot tube. Once these waves stabilize for fully supersonic flow ($M > 1.2$), the comparison between computed and experimental results becomes reasonable. Because of this uncertainty, we did not attempt computations in the transonic regime ($0.9 \leq M \leq 1.2$) for the present study. Additionally, for supersonic aircraft, flight through the transonic regime is a short transitionary phenomenon (for various reasons) and not an extended duration activity, therefore, transonic

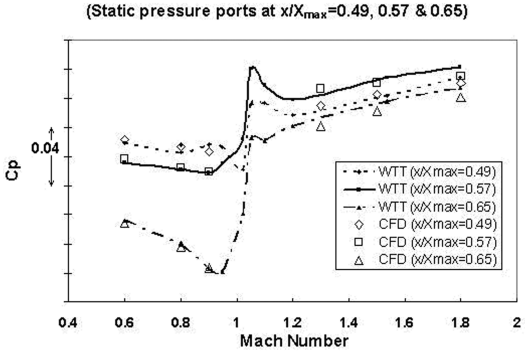

Fig. 6 Comparison of computed and experimental *Cp* behavior at static pressure port locations $x/X_{\max} = 0.49$, 0.57, and 0.65 for a representative pitot tube.

characteristics of the pitot tube are normally not emphasized by designers.

The actual tested pitot tube has a single total pressure port of 4-mm diameter at its forward tip and a number of small static pressure ports [1] at different axial locations ($x/X_{\max} = 0.49$, 0.57, and 0.65) on its surface in the compensation region. For CFD analysis, the total pressure port was not modeled, because we have verified in an earlier study [14] that the spillage effect from such a pressure port has negligible effect on pitot tube surface pressure characteristics significantly downstream ($x/X_{\max} > 0.4$) from the tip. This conclusion is reinforced by the results shown in Fig. 6.

IV. Results and Discussion

To cover the flight envelope of a supersonic aircraft, computations were carried out at Mach numbers of 0.6, 0.8, 0.9, 1.2, 1.6, and 1.8 for all analyzed pitot tubes. From our experience (discussed earlier in the paper), we found it difficult to correlate computed results to practical situations in the transonic regime (Fig. 6). Therefore, computations were not attempted between Mach numbers 0.9 and 1.2.

The basic flowfield around the pitot tube for all cases of the present study consists of freestream flow being modified by the presence of the tube. The flow adjacent to the pitot tube generally follows its contour, whereas far away, it merges with the freestream flow. There is no separation/recirculation region near the pitot tube, therefore, streamline or vector plots are not necessary to visualize this simple flowfield.

A. Simplified Compensation Region Profile Based on Conical Segments

We analyzed a number of simplified pitot tube profiles based on conical segments, as discussed earlier in this paper (Sec. II, "Development Methodology of Proposed Compensation Region Profile"). Only the most promising (fine-tuned) arrangement of the simplified profile is discussed here. The pressure coefficient Cp variation in the vicinity of the pitot tube compensation region is shown in Figs. 7 and 8 for freestream Mach numbers of 0.6 and 1.4, respectively. Because the flow in Fig. 7 is subsonic ($M = 0.6$), the pressure variations ahead of the pitot tube are evident. Rapid changes in the surface Cp in the vicinity of conical segment junctions is also evident. At supersonic speeds, the flow reacts to the presence of the pitot tube via a conical shock wave, as seen in Fig. 8. Large pressure changes in the shock/expansion waves pinned to the sharp corners formed by conical segments are evident. The pressure adjacent to the pitot tube surface extends to the surface itself, indicating no pressure variation normal to the surface in the viscous boundary layer. Detailed Cp variation along the pitot surface is not evident from Figs. 7 and 8 and is discussed next in this paper.

The computed Cp variation along the surface of the pitot tube with simplified compensation region is shown in Figs. 9 and 10 at

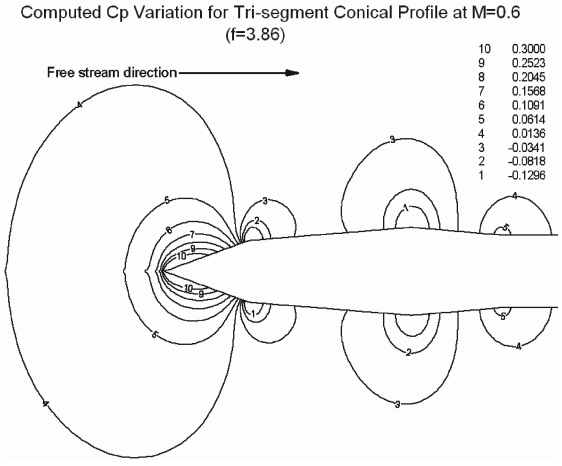

Fig. 7 Computed subsonic *Cp* variation in the vicinity of the pitot tube with a simplified conical segment profile ($M = 0.6$ and $f = 3.86$).

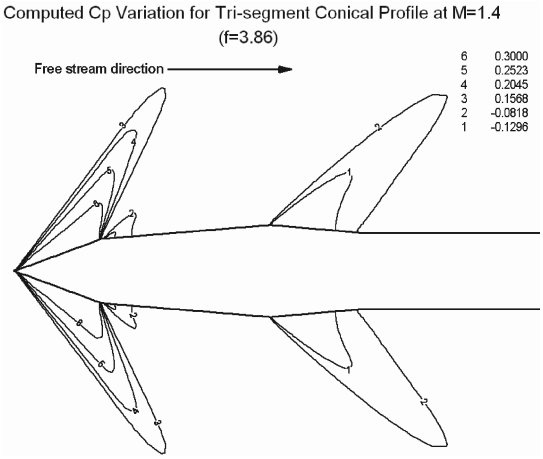

Fig. 8 Computed supersonic *Cp* variation in the vicinity of the pitot tube with a simplified conical segment profile ($M = 1.4$ and $f = 3.86$).

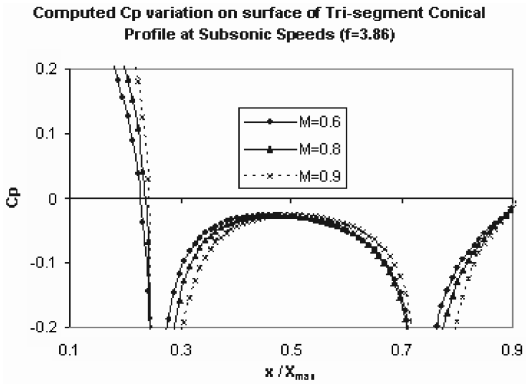

Fig. 9 Computed surface *Cp* variation for a simplified compensation profile pitot tube at subsonic Mach numbers ($f = 3.86$).

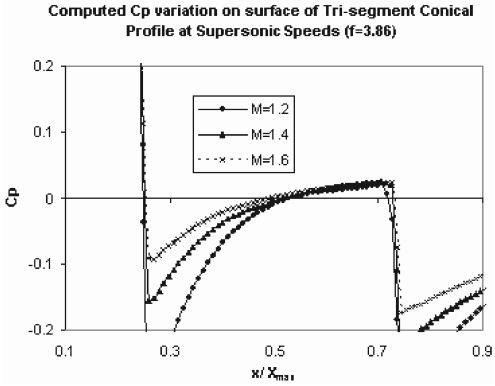

Fig. 10 Computed surface *Cp* variation for a simplified compensation profile pitot tube at supersonic Mach numbers ($f = 3.86$).

subsonic and supersonic Mach numbers, respectively. The rapid pressure variation in the vicinity of sharp corners formed at the interface of conical segments (i.e., $x/X_{\max} = 0.25$ and $x/X_{\max} = 0.74$) are evident from these figures. This particular combination of conical segments gives negative Cp values at subsonic Mach numbers around axial location $x/X_{\max} = 0.5$ (Fig. 9), whereas at approximately the same axial location, it gives nearly zero Cp values at supersonic Mach numbers (Fig. 10). From a practical application aspect, a static pressure port located at $x/X_{\max} = 0.5$ is acceptable, because it is not too close to the pitot tube front tip to be influenced by spillage flow from the total pressure port. Another positive aspect of this particular combination of conical segments seen in Figs. 9 and 10 is the small local gradient of Cp at the axial

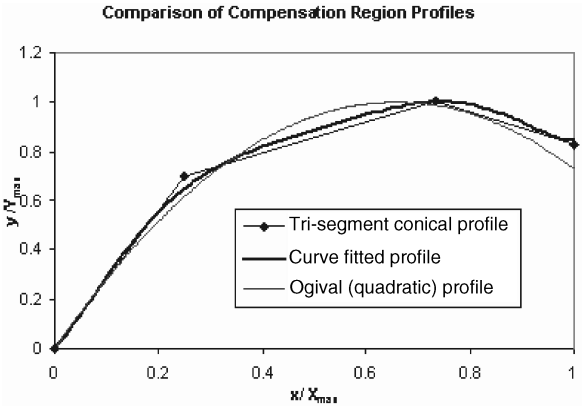

Fig. 11 Comparison of various compensation region profiles.

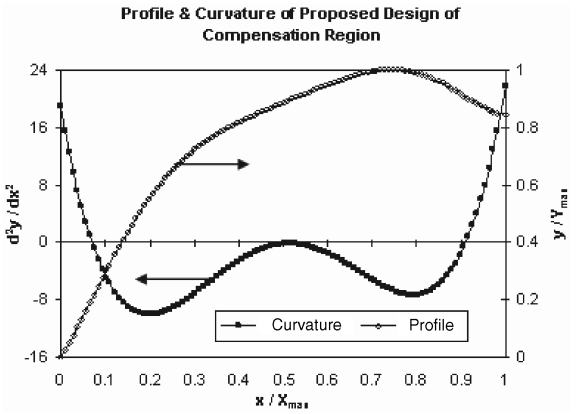

Fig. 12 Profile and curvature of the higher-order polynomial-based compensation region.

location of interest ($x/X_{\max} = 0.5$). This aspect becomes clear once Figs. 9 and 10 are compared with Fig. 2, which shows the surface Cp behavior of the ogival pitot tube. We found further refinement possible based on this feature of the simplified profile.

B. Refined Compensation Region Profile Based on Higher-Order Polynomials

The refinement process included smoothing out the sharp edges formed at the conical interfaces so that the pressure peaks shown in Figs. 9 and 10 at $x/X_{\max} = 0.25$ and $x/X_{\max} = 0.74$ diffuse axially, with anticipated further reduction in subsonic Cp at $x/X_{\max} = 0.5$. In the supersonic regime, this refinement was expected to reduce the local Cp gradient further at the desired axial location ($x/X_{\max} = 0.5$).

We evaluated different higher-order polynomials for smoothing the simplified profile (conical segments). The final higher-order polynomial fitted compensation region profile is shown in Fig. 11. The simplified (conical segments) and the ogival (quadratic polynomial) compensation region profiles are also included for comparison. Adequate smoothing of the sharp edges of the conical segments, while retaining the overall shape characteristics, is evident for the curve-fitted profile. We also evaluated the curvature of the higher-order polynomial-based profile, as shown in Fig. 12. This was necessary to ensure that no undesirable surface "wiggles" exist on the compensation region. As can be seen in Fig. 12, the curve-fitted profile has negative curvature, except for small regions at the ends.

We computed the flowfield and the corresponding pressure distribution around the proposed design pitot tube for verification of desirable Cp characteristics in both subsonic and supersonic regimes. The basic flowfield in both subsonic and supersonic regimes is similar to the simplified (conical segments) pitot tube discussed earlier in this paper. A representative Cp distribution in the subsonic regime is shown in Fig. 13 at $M = 0.6$ for the proposed design pitot

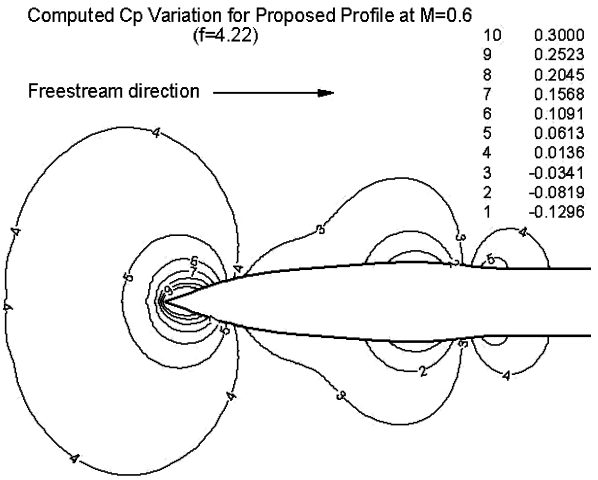

Fig. 13 Computed Cp distribution in the vicinity of the proposed design pitot tube ($M = 0.6$ and $f = 4.22$).

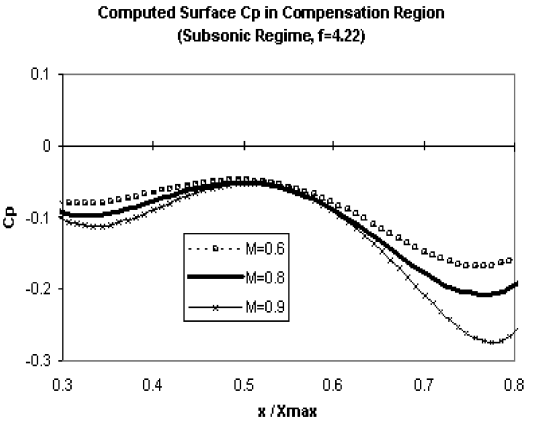

Fig. 14 Subsonic Cp distribution on the surface of the compensation region of the proposed design pitot tube ($f = 4.22$).

tube. The rapid pressure changes in the vicinity of conical segment junctions, as seen earlier in Fig. 7, have axially diffused. A similar trend is observed in the supersonic regime, because the concentrated expansion waves associated with conical segment junctions (Fig. 8) are also more spread out axially for the proposed design. The figure for supersonic Cp distribution in the vicinity of the pitot tube is omitted, for brevity.

Detailed surface Cp distribution of the proposed design at both subsonic and supersonic Mach numbers is shown in Figs. 14 and 15, respectively. Gradual pressure variations on the surface of the pitot

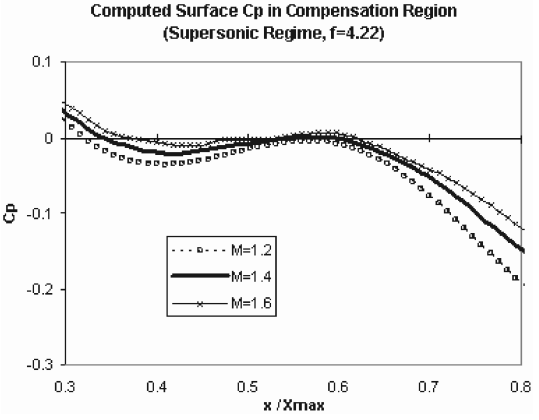

Fig. 15 Supersonic Cp distribution on the surface of the compensation region of the proposed design pitot tube ($f = 4.22$).

tube are apparent. This is in contrast to pressure peaks observed for the simplified compensation region case, shown in Figs. 9 and 10. For the supersonic case (Fig. 15), the surface Cp approaches zero value at $x/X_{\max} = 0.56$. At this axial location, the local gradient of the surface Cp is near zero as well, which means that within a reasonable range of $x/X_{\max}$ (about 0.55–0.57), the supersonic Cp would remain nearly zero. This feature of the proposed design is very attractive, because it affords a significant tolerance in placing the static pressure port on the surface of the pitot tube for practical application. At subsonic speeds (Fig. 14), a consistent negative Cp value is achieved over the surface of the compensation region. At $x/X_{\max} = 0.56$, a Cp value of about -0.06 is achieved, which is typical of medium-to-small supersonic fighter aircraft at subsonic speeds some distance ahead of their fuselage, where a pitot tube is normally installed [1,14]. A desirable aspect of the proposed design is that at $x/X_{\max} = 0.56$, the surface Cp value is not very sensitive to Mach number, as seen in Figs. 14 and 15. Moreover, at this axial location, the local Cp gradient is not large. Therefore, a single static pressure port located at $x/X_{\max} = 0.56$ would give nearly zero compensation at supersonic speeds (desirable), while maintaining a reasonable level (Cp value of about -0.06) of compensation in the subsonic regime. So far we have discussed the proposed design pitot tube having a fineness ratio $f = 4.22$. At other fineness ratios, the subsonic Cp values at $x/X_{\max} = 0.56$ are expected to change significantly, whereas in the supersonic regime, some variations may also occur. This aspect is discussed for the practical application of the proposed design pitot tube.

V. Practical Application of Proposed Design Pitot Tube

A robust pitot tube design should be capable of compensating for a wide range of subsonic Cp position error values corresponding to various types and sizes of aircraft and, at the same time, maintaining near-zero Cp compensation at supersonic speeds. For this purpose, the nondimensional proposed design profile (Figs. 11 and 12) was stretched. This nondimensional stretching resulted in compensation regions of various fineness ratios. We computationally evaluated the Cp characteristics of these resultant pitot tubes (different fineness ratios) at subsonic and supersonic speeds. The results of our computations at the proposed static port location of $x/X_{\max} = 0.56$ is shown in Fig. 16. Reducing the fineness ratio of the nondimensional profile results in dimensional increase in profile curvature and vice versa, therefore, the surface Cp at subsonic speeds has greater negative value for lower values of f and lesser negative value for higher values of f, as seen in Fig. 16. At supersonic speeds, the effect of the fineness ratio on the surface Cp at $x/X_{\max} = 0.56$ is negligible, which retains the near-zero value. Fineness ratio variation from three to five results in subsonic Cp error compensation capability from 0.04 to 0.1, as seen in Fig. 16. This capability is deemed sufficient for most practical applications [1].

A nondimensional parameter pressure coefficient fineness ratio (i.e., $Cp * f$, for the same upstream Mach number) is suggested by

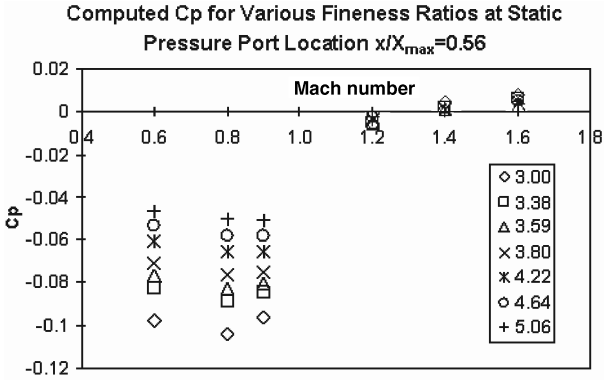

Fig. 16 Cp vs Mach number behavior for various fineness ratios at static pressure port location $x/X_{\max} = 0.56$.

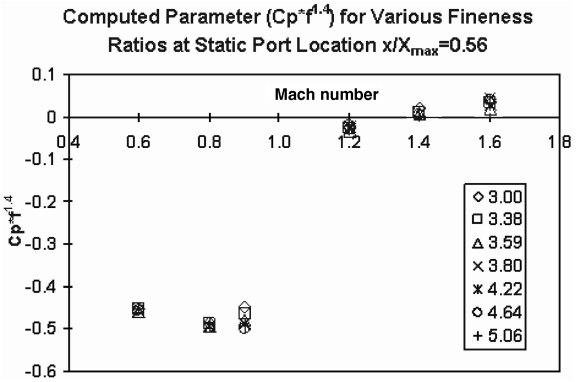

Fig. 17 Modified parameter $Cp * f^{1.4}$ vs Mach number behavior for various fineness ratios at static pressure port location $x/X_{\max} = 0.56$.

similarity rules based on linearized compressible flow theory that should correlate the data presented in Fig. 16. However, we found that an alternate parameter with modified power of the fineness ratio (i.e., $Cp * f^{1.4}$) correlates the data presented in Fig. 16 better. This is due to limitation of the linearized compressible flow theory, which assumes small axial (x direction) and radial (y direction) perturbation velocities, whereas in the real case, these velocities may not be small. This is especially true for low-to-moderate fineness ratios such as the present case (f varies from three to five, Fig. 16). In this situation, the influence of f is expected to be larger (power of f being 1.4 instead of 1.0 in the nondimensional parameter) than that predicted by linearized compressible flow theory. The data correlated by using the parameter $Cp * f^{1.4}$ are presented in Fig. 17. Very good data correlation is observed at $M = 0.6$ and 0.8. However, at $M = 0.9$, some variations in correlated data are evident for low fineness ratios ($f = 3.00$ and 3.38), probably due to earlier onset of transonic effects because of the combination of higher curvature (low value of f) and high subsonic Mach number.

Figure 17 can be conveniently used instead of Fig. 16 to apply the results of the present work to a practical situation. From Fig. 17, we get the value of the parameter $Cp * f^{1.4}$ as

$$Cp * f^{1.4} = |-0.454| \quad \text{at } M = 0.6 \tag{1}$$

$$Cp * f^{1.4} = |-0.49| \quad \text{at } M = 0.8 \tag{2}$$

For any practical application, the required level of subsonic compensation (Cp error value) is known from CFD analysis or wind-tunnel tests. Corresponding to this Cp error value, f can be determined from Eq. (1) or Eq. (2) for $0.6 \le M \le 0.8$ (interpolate, if necessary) or from Fig. 16 directly for $0.8 < M \le 0.9$. Knowing the value of f, we can now refer to Figs. 11 and 12 to find the dimensional profile, because the pitot tube cylindrical straight end radius corresponding to $y/Y_{\max} = 0.84$ at $x/X_{\max} = 1$ is known or can be chosen based on other design considerations (structural, etc.). Thus, $Y_{\max}$, $X_{\max}$, and dimensional profile details are now known for the value of Cp error that needs to be aerodynamically compensated in the subsonic regime. At supersonic Mach numbers ($1.2 < M < 2$), the dimensional profile would automatically give the desired near-zero compensation (Fig. 16).

We have verified this methodology to effectively compensate for position error in Cp of up to $+0.1$ (most practical applications), as shown in Fig. 16. We may also be able to compensate for higher values of Cp error (greater than 0.1) by this methodology but that requires further verification. However, Cp error values lower than 0.04 can be compensated by this methodology without further analysis, because that requires larger values of the fineness ratio ($f > 5$), which makes the flow behavior in the vicinity of the pitot tube less susceptible to transonic effects, even at $M = 0.9$.

In addition to the profile information, the physical pitot tube needs a pitot (total) pressure port at the pitot tube tip as well as a static pressure port at $x/X_{\max} = 0.56$. The physical dimension and shape of

these ports and their azimuthal orientation (static pressure ports only) for nonzero AOA and β can be found from [1]. We have discussed earlier in this paper that the spillage flow from a correctly dimensioned pitot pressure port at the pitot tube tip does not effect the Cp behavior in the compensation region beyond about $x/X_{\max} > 0.4$, where the static pressure port is located ($x/X_{\max} = 0.56$) for the proposed pitot tube.

The overall improvement of the proposed design compared with an ogival pitot tube (Fig. 1) can be gauged by comparing the results of Fig. 2 with those of Figs. 14–16 for a single static pressure port located at $x/X_{\max} = 0.46$ and $x/X_{\max} = 0.56$ for the ogival and the proposed pitot tubes, respectively. At these axial locations, the supersonic Cp is near zero for both the tubes. At $M = 1.4$, a variation of $\pm 5\%$ (of $X_{\max}$) in the axial location $x/X_{\max}$ of the static pressure port causes a corresponding variation in measured Cp of about 50 and 2% (of the subsonic value) for the ogival and proposed pitot tubes, respectively. This shows that the ogival pitot tube is much more sensitive to tolerances in static pressure port location than the proposed pitot tube for application on supersonic aircraft. To reduce this error in the ogival pitot tube, multiple axially distributed static pressure ports are generally used, as discussed earlier in this paper. The proposed pitot tube does not suffer from such shortcoming.

VI. Conclusions

An aerodynamic compensation pitot tube design for supersonic aircraft is presented in this paper. The proposed design has a compensation region defined by a higher-order polynomial that improves upon the Cp compensation characteristics of the ogival (quadratic polynomial) pitot tube by modifying the surface pressure distribution. The improved compensation characteristics are achieved at a single static pressure port located at $x/X_{\max} = 0.56$. The proposed design pitot tube is able to compensate for position error in Cp of up to $+0.1$ in the subsonic regime ($M < 0.9$) by nondimensional stretching of the basic profile, while maintaining near-zero Cp in the supersonic regime ($1.2 < M < 2$). The data of the present study are correlated by a parameter $Cp * f^{1.4}$ at the static pressure port location $x/X_{\max} = 0.56$, which makes practical application of the present work convenient.

Acknowledgments

Adnan Latif gratefully acknowledges the MS thesis research grant provided by the National University of Sciences and Technology. Jehanzeb Masud would like to acknowledge the discussions that took place with Chinese engineers on air data sensors.

References

[1] Garcy, W., "Measurement of Aircraft Speed and Altitude," NASA Reference Publication 1046, 1980.
[2] Letko, W., "Investigation of the Fuselage Interference on a Pitot-Static Tube Extending Forward from the Nose of the Fuselage," NACA TN-1496, 1947.
[3] Ritchie, V. S., "Several Methods for Aerodynamic Reduction of Static-Pressure Sensing Errors for Aircraft at Subsonic, Near-Sonic, and Low Supersonic Speeds," NASA TR R-F18, 1959.
[4] Swafford, T. W., Bomba, J., and Daiber, M. P., "Computational Evaluation of Compensated Pitot-Static Probes Using the Euler Equations," AIAA Paper 1995-1839, June 1995.
[5] Lao, S., and Bao, Y., "Computation of Transonic Aerodynamically Compensating Pitot Tube," *Journal of Aircraft*, Vol. 25, No. 6, 1987, pp. 544, 560.
[6] Schreier, S., "Two and Three Dimensional Steady Supersonic Flow," *Compressible Flow*, Wiley, New York, 1982, pp. 133–200.
[7] "Equations, Tables, and Charts for Compressible Flow," NACA Rept. 1135, 1953.
[8] FLUENT, Computational Fluid Dynamics, Software Package, Ver. 6.2.16, Fluent Inc., Lebanon, NH, 2004.
[9] GAMBIT, Geometry and Mesh Generation Software Package, Ver. 2.2.30, Fluent Inc., Lebanon, NH, 2005.
[10] FLUENT, Computational Fluid Dynamics Software Package User Guide, Ver. 6.2.16, Fluent Inc., Lebanon, NH, 2004.
[11] White, F. M., "Compressible Boundary Layer Flow," *Viscous Fluid Flow*, 2nd ed., McGraw–Hill, New York, 1991, pp. 500–562.
[12] Lauder, B. E., and Spalding, D. B., *Lectures in Mathematical Models of Turbulence*, Academic Press, London, 1972.
[13] Spalarat, P., and Allmaras, S., "A One-Equation Turbulence Model for Aerodynamic Flows," AIAA Paper 92-0439, 1992.
[14] Latif, A., "Design and Integration of Aerodynamic Compensating Pitot-Static Tube for a Supersonic Aircraft," M.S. Thesis, Aerospace Engineering Dept., College of Aeronautical Engineering, National Univ. of Sciences and Technology, Risalpur, Pakistan, 2005.